AIAA SciTech Forum
8–12 January 2018, Kissimmee, Florida
2018 AIAA Atmospheric Flight Mechanics Conference

10.2514/6.2018-0018

Path Constraint Regularization in Optimal Control Problems using Saturation Functions

Thomas Antony* and Michael J. Grant †
Purdue University, West Lafayette, Indiana 47907-2045

State-of-the-art direct and indirect methods face significant challenges when solving large scale constrained trajectory optimization problems. One of the main challenges is the difficulty in handling path inequality constraints, particularly in the case of indirect methods. A methodology called the Integrated Control Regularization Method (ICRM) is developed for incorporating path inequality constraints into optimal control problems using saturation functions. This new method removes the need for multiple constrained and unconstrained arcs when dealing with path constraints and produces a single smooth constrained trajectory. Furthermore, it also addresses the issue of transcendental control law equations by re-formulating the problem so that it can be solved by existing numerical solvers for Two-Point Boundary Value Problems (TPBVPs). The capabilities of ICRM are demonstrated by using it to solve some representative constrained trajectory optimization problems.

Nomenclature

$\dot{Q}$	Convection heat rate at stagnation point, W/m^2	H	Hamiltonian
		h	Altitude, m
$\mathbf{u}$	Control vector	h_s	Scale height, m
$\mathbf{x}$	State vector	m	Mass, kg
A_{ref}	Reference area, m^2	R_E	Radius of the Earth, m
C_D	Coefficient of Drag	r_n	Nose radius, m
C_L	Coefficient of Lift	V	Velocity, m/s
α	Angle of Attack, rad	$\mathbf{\Phi}_f$	Terminal boundary conditions
γ	Flight path angle, rad	μ	Standard gravitational parameter, m^3/s^2
λ	Costate vector	ρ_0	Atmospheric density at sea-level, kg/m^3
$\mathbf{\Phi}_0$	Initial boundary conditions	θ	Downrange angle, rad

I. Introduction

Modern research in trajectory optimization and mission design has been focused on pseudo-spectral and other direct methods for the last few decades.[1–4] Indirect methods that leverage calculus of variations are

*PhD Candidate, School of Aeronautics and Astronautics, AIAA Student Member, tantony@purdue.edu
†Adjunct Assistant Professor, School of Aeronautics and Astronautics, AIAA Senior Member, mjgrant@purdue.edu

often cited as being too impractical or difficult to apply to real-world problems owing to many reasons.[2] However, prior work has shown that it is possible to overcome many of these challenges using a continuation methodology to solve constrained trajectory optimization problems.[5] Indirect methods produce solutions that satisfy the necessary conditions of optimality, guaranteeing a local minimum. Moreover, indirect methods convert the optimization problem into a boundary value problem (BVP) that can be solved using highly parallel methods with fast convergence.[6]

One of the drawbacks of indirect methods is the difficulty in incorporating path inequality constraints.[1] These methods require that in the presence of path constraints, the trajectories must be separated into multiple arcs introducing interior-point boundary conditions.[7] It is difficult to generate an initial guess for the sequence of unconstrained and constrained arcs a-priori as well as to obtain guesses for these boundary conditions which may include discontinuities. This can be mitigated to a certain extent using a continuation methodology as demonstrated in Ref. 5. However, this approach still faces challenges when dealing with multiple constraints involving a large number of states and constrained arcs.

A far simpler method is presented in Ref 8, in which state and control inequality constraints can be systematically incorporated into an optimal control problem. This method retains the trajectory as a single arc even in the presence of path constraints. The original formulation of regularized path constraints required the use of a custom numerical solver due to extra algebraic equations adjoined to the boundary value problem (BVP) that do not have closed form solutions.[8] The author of Ref. 8 developed a numerical solver based on collocation in order to address this. This solver may not be suitable for parallelization and likely suffers from scalability issues as the problem size grows.

To overcome these challenges, a new way of formulating constrained optimal control problems is proposed. In this method, the optimal control law is obtained, not by analytically solving algebraic equations in the traditional manner, but by converting the algebraic conditions into extra differential equations. This allows the control variables to be numerically integrated rather than directly obtaining them from closed form control laws. While differentiating an existing equation and numerically integrating it may seem counter-intuitive, it greatly simplifies the process of solving complicated optimal control problems as described in the subsequent sections.

Using saturation functions to regularize path constraints and numerically integrating the control, greatly change and simplify the general approach to solving large-scale constrained trajectory optimization problems. This method is termed as the Integrated Control Regularization Method (ICRM).

II. Overview of Optimal Control Theory

A. Necessary Conditions of Optimality

Consider an optimal control problem as shown below:

$$\text{Min } J = \phi(\boldsymbol{x}(t_f), t_f) + \int_{t_0}^{t_f} L(\boldsymbol{x}, \boldsymbol{u}, t)\,\mathrm{d}t \tag{1}$$

$$\text{Subject to :}$$

$$\dot{\boldsymbol{x}} = \boldsymbol{f}(\boldsymbol{x}, \boldsymbol{u}, t) \tag{2}$$

$$\boldsymbol{\Phi}_0(\boldsymbol{x}(t_0), t_0) = 0 \tag{3}$$

$$\boldsymbol{\Phi}_f(\boldsymbol{x}(t_f), t_f) = 0 \tag{4}$$

$$t_0 = 0$$

Indirect methods optimize the cost functional J shown in Eq. (1) by formulating a multi-point boundary value problem that represents the necessary conditions of optimality. If these boundary conditions are satisfied, the solution will be locally optimal in the design space. In order to formulate this BVP, the dynamic equations of the system are augmented with a set of costates, and the necessary conditions of optimality are formulated by applying the Euler-Lagrange equation.[9]

The Hamiltonian is defined as shown in Eq. (5), where $\boldsymbol{\lambda}$ is the costate vector with its corresponding dynamic equations defined in Eq. (6). The optimal control law, $\boldsymbol{u}(t)$ is obtained as a function of the states and costates by solving Eq. (7). The initial and terminal boundary conditions on the costates are specified

in Eqs. (8) and (9), where ν_0 and ν_f are sets of undetermined parameters which are used to adjoin these boundary conditions to the cost functional. The time of flight of the trajectory is determined by the free-final time condition in Eq. (10). The necessary conditions of optimality are defined by Eqs.(6–10), and they form a well-defined Two-Point Boundary Value Problem (TPBVP) that can be solved rapidly using the shooting method.

$$H = L(x,u,t) + \boldsymbol{\lambda}^T(t)\boldsymbol{f}(\boldsymbol{x},\boldsymbol{u},t) \tag{5}$$

$$\dot{\boldsymbol{\lambda}} = -\frac{\partial H}{\partial \boldsymbol{x}} \tag{6}$$

$$\frac{\partial H}{\partial \boldsymbol{u}} = 0 \tag{7}$$

$$\boldsymbol{\lambda}(t_0) = \boldsymbol{\nu_0}^T \frac{\partial \boldsymbol{\Phi}_0}{\partial \boldsymbol{x}(t_0)} \tag{8}$$

$$\boldsymbol{\lambda}(t_f) = \left(\frac{\partial \phi}{\partial \boldsymbol{x}(t_f)} + \boldsymbol{\nu_f}^T \frac{\partial \boldsymbol{\Phi}_f}{\partial \boldsymbol{x}(t_f)}\right) \tag{9}$$

$$\left(H + \frac{\partial \phi}{\partial t} + \boldsymbol{\nu_f}^T \frac{\partial \boldsymbol{\Phi}_f}{\partial t}\right)_{t=t_f} = 0 \tag{10}$$

B. Path Constraints

The presence of path constraints further complicates the boundary conditions by introducing corner conditions in certain costates and effectively splitting the trajectory into multiple arcs. Consider a one sided path constraint of the form shown in Eq. (11). To obtain the control history for the constrained arc, time derivatives of the path constraints are taken until the control variable appears explicitly. If this happens with the q^{th} derivative, the Hamiltonian is augmented as shown in Eq. (12), and the control law for the constraint boundary arc is obtained by solving $\boldsymbol{S}^{(q)} = 0$.

$$\boldsymbol{S}(\boldsymbol{x},t) \leq 0 \tag{11}$$

$$H = L + \boldsymbol{\lambda}^T \boldsymbol{f} + \boldsymbol{\mu}^T \boldsymbol{S}^{(q)} \tag{12}$$

The addition of path constraints also modifies the dynamic equations of the costates along the constrained arcs as shown in Eq. (13), where the multipliers $\boldsymbol{\mu}$ are calculated by solving Eq. (14).

$$\dot{\boldsymbol{\lambda}} = -\frac{\partial H}{\partial \boldsymbol{x}} = -L_x - \boldsymbol{\lambda}^T \boldsymbol{f}_x - \boldsymbol{\mu}^T \boldsymbol{S}_{\boldsymbol{x}}^{(q)} \tag{13}$$

$$\frac{\partial H}{\partial \boldsymbol{u}} = L_u + \boldsymbol{\lambda}^T \boldsymbol{f}_u + \boldsymbol{\mu}^T \boldsymbol{S}_{\boldsymbol{u}}^{(q)} = 0 \tag{14}$$

The states are continuous at the entry (t_1) and exit (t_2) of the constrained arc as shown in Eq. (15). Corner conditions on costates are chosen such that the costates are continuous at the exit of the constrained arc as shown in Eq. (16). The tangency conditions described in Eq. (17) and corner conditions in Eq. (18) and Eq. (19) apply at the entry point of the constrained arc.

$$\begin{aligned} \boldsymbol{x}(t_1{}^+) &= \boldsymbol{x}(t_1{}^-) \\ \boldsymbol{x}(t_2{}^+) &= \boldsymbol{x}(t_2{}^-) \end{aligned} \tag{15}$$

$$\begin{aligned} \boldsymbol{\lambda}(t_2{}^+) &= \boldsymbol{\lambda}(t_2{}^-) \\ H(t_2{}^+) &= H(t_2{}^-) \end{aligned} \tag{16}$$

$$\boldsymbol{N}(\boldsymbol{x},t) = \begin{bmatrix} S(\boldsymbol{x},t) \\ S^{(1)}(\boldsymbol{x},t) \\ S^{(2)}(\boldsymbol{x},t) \\ . \\ . \\ . \\ S^{(q-1)}(\boldsymbol{x},t) \end{bmatrix} \tag{17}$$

$$\boldsymbol{\lambda}({t_1}^+) = \boldsymbol{\lambda}({t_1}^-) + \boldsymbol{\Pi}^T \boldsymbol{N}_{\boldsymbol{x}} \tag{18}$$

$$H({t_1}^+) = H({t_1}^-) + \boldsymbol{\Pi}^T \boldsymbol{N}_t \tag{19}$$

C. Need for a new approach

The application of the method described in this section on optimal control problems with path constraints hinges on a-priori knowledge of several factors. It requires the knowledge of the number and sequence of constrained and unconstrained arcs. The method also needs the designer to provide an initial guess for the interior point conditions on the costates which might be very difficult. These challenges can be highly impractical to overcome for anything but the simplest problems. The number of arcs and interior boundary conditions can grow very fast once we add multiple path constraints to the problem that may be active and inactive multiple times over the course of the trajectory, which in turn complicates the formulation and the numerical solution of the MPBVP.

There has been some prior work that attempts to solve these issues. Refs. 10 and 11 describe a method that uses trigonometric functions to regularize control constraints. This method also helps avoid transcendental equations when the control is of trigonometric form. However, it is not a general solution as its application is limited to certain classes of problems. All these challenges motivate the need to develop a new approach that can incorporate path constraints efficiently while retaining the advantages of using indirect methods for trajectory optimization.

III. Integrated Control Regularization Method

A. Regularization of Path Inequality and Control Constraints

In the original work,[8] it was shown that path constraints can be regularized by representing them as smooth saturation functions. An intrinsic property of the saturation function method is that the constraints cannot be violated at any point of the trajectory during the numerical solution process since they are incorporated into the new optimal control problem (OCP). As an example, consider a general optimal control problem with a path constraint as follows:

$$\begin{aligned} \text{Min } J &= \phi(\mathbf{x}(T),T) + \int_0^T L(t,\mathbf{x},\mathbf{u})\ dt \\ \dot{\mathbf{x}} &= f(t,\mathbf{x},\mathbf{u}), & \Phi(\mathbf{x}(0),\mathbf{x}(T)) &= 0 \\ c_i(\mathbf{x}) &\in [c_i^-, c_i^+], & i &= 1\dots p \end{aligned} \tag{20}$$

where $c_i(\mathbf{x})$ represents the path constraints in the problem. The constraint is replaced by a suitable saturation function, ψ:

$$c_i(\mathbf{x}) = \psi(\xi_{i,1}), i = 1\dots p \tag{21}$$

Eqn. (21) is successively differentiated w.r.t time, and new coordinates, $\dot{\xi}_{i,j} = \xi_{i,j+1}$, are introduced, until the control variable appears. For example, if $c_i(\mathbf{x})$ is of order 2:

$$\begin{aligned} c^{(1)}(\mathbf{x}) &= \psi'\dot{\xi}_{i,1} & &:= h_1, & \dot{\xi}_{i,1} &= \xi_{i,2} \\ c^{(2)}(\mathbf{x}) &= \psi''\xi_{i,2}^2 + \psi'\dot{\xi}_{i,2} & &:= h_2, & \dot{\xi}_{i,2} &= u_{e1} \end{aligned} \tag{22}$$

Finally, an equality constraint, $c_i^{(q)}(\mathbf{x}) - h_q = 0$ is also added to the problem along with an added term $\int_0^T \epsilon u_{e1}^2 dt$ to the path cost, where u_{e1} is a new control variable, $\xi_{i,j}$ are new state variables, ϵ is a regularization parameter and q is the order of the constraint. The resulting extended optimal control problem which incorporates the path constraints is then solved using a suitable numerical method. It is to be noted that while the size of the problem has increased during this process, the use of parallel BVP solvers mitigates this to a certain extent.[6]

B. Candidate Saturation Functions

There are many functions that can be used as saturation functions for path constraint regularization. Some of the common examples are the sigmoid, arc-tangent, and hyperbolic tangent functions. Ref. 8 suggests the following saturation functions as candidates for path constraint regularization depending on the type of constraint.

For one-sided constraints with an upper bound ($c(x) \leq c^+$) or a lower bound ($c(x) \geq c^-$), Eqs. (23) or (24) respectively may be used as saturation functions.

$$\psi(\xi) = c^+ - \exp(-\xi) \tag{23}$$

$$\psi(\xi) = c^- + \exp(\xi) \tag{24}$$

For two-sided functions, such as $c^- \leq c(x) \leq c^+$, the following function based on the sigmoid function is recommended by the authors of Ref. 8. Eq. (25) is formulated so that the resulting function has a slope of one at $\xi = 0$.

$$\psi(\xi) = c^+ - \frac{c^+ - c^-}{1 + \exp(s\xi)}, s = \frac{4}{c^+ - c^-} \tag{25}$$

C. Differential Optimal Control Law

The standard procedure in indirect methods is to define a Hamiltonian, H, that incorporates all the dynamic equations and some mathematical entities called costates along with any path-cost and equality constraints in the problem. H is then used to obtain a closed-form solution for the control variables ($\mathbf{u}$) by solving an algebraic equation ($\frac{\partial H}{\partial u} = 0$), thereby eliminating them from the overall problem to obtain a BVP of the form shown in Eqn. (26). However, the control law equation may have multiple solutions, requiring further effort to determine which one is optimal. It is also possible that the control equation may have no closed form solution, requiring the use of numerical root-solving functions within the dynamic equations, which is highly inefficient.

$$\frac{dx}{dt} = f(t, \mathbf{x}),\ b(\mathbf{x}(t_0), \mathbf{x}(t_f)) = 0 \tag{26}$$

The application of saturation functions for regularization of path constraints results in a BVP of the form shown in Eqn. (27). In such a BVP, the control law in Eqn. (27b) consists of transcendental equations that generally have no closed form solution. Such BVPs are called Differential-Algebraic Equation Boundary Value Problems (DAE-BVP). As mentioned before, in Ref. 8, a custom numerical solver based on collocation was developed to solve these BVPs.

$$\frac{dx}{dt} = f(t, \mathbf{x}, \mathbf{u}),\ b(\mathbf{x}(t_0), \mathbf{x}(t_f)) = 0 \tag{27a}$$

$$g(t, \mathbf{x}, \mathbf{u}) = 0 \tag{27b}$$

Solving such BVPs is a non-trivial task in general and has been extensively examined in literature.[12–17] References 18,19 and 20 discuss numerical methods for solving a certain class of such DAEs called semi-explicit DAEs. Based on these prior works, we propose a reformulation of the DAE-BVP as shown in Eqn. (27), that retains the control variables, $\mathbf{u}$ in the boundary value problem rather than eliminating them. Eqn. (27b) can then be differentiated to obtain dynamic equations ($\dot{\mathbf{u}}$) for the control variables as shown in Eqn. (28).

$$\begin{aligned} 0 &= \partial_x g(t,\mathbf{x},\mathbf{u})\dot{\mathbf{x}} + \partial_u g(t,\mathbf{x},\mathbf{u})\dot{\mathbf{u}} + \partial_t g(t,\mathbf{x},\mathbf{u}) \\ \implies \partial_u g(t,\mathbf{x},\mathbf{u})\dot{\mathbf{u}} &= -\partial_x g(t,\mathbf{x},\mathbf{u})\dot{\mathbf{x}} - \partial_t g(t,\mathbf{x},\mathbf{u}) \end{aligned} \tag{28}$$

The original algebraic constraint in Eqn. (27b) is then added as a boundary condition at either the initial or terminal point to obtain a well-formed two-point boundary value problem in Eqn. (29). This is called "index-reduction" of a DAE and is one of the strategies used for solving such problems.

$$\frac{dx}{dt} = f(t,\mathbf{x},\mathbf{u}) \tag{29a}$$

$$\partial_u g(t,\mathbf{x},\mathbf{u})\dot{\mathbf{u}} = -\partial_x g(t,\mathbf{x},\mathbf{u})\dot{\mathbf{x}} - \partial_t g(t,\mathbf{x},\mathbf{u}) \tag{29b}$$

$$g(t_0,\mathbf{x}(t_0),\mathbf{u}(t_0)) = 0, \quad b(\mathbf{x}(t_0),\mathbf{x}(t_f)) = 0 \tag{29c}$$

IV. Test Cases

A. Constrained Brachistochrone Problem

A proof of concept for ICRM was tested by applying it to the classical Brachistochrone problem modified by adding a path constraint.

Problem Statement:

$$\text{Min } T \tag{30a}$$

$$\text{Subject to :}$$

$$\dot{x} = v\cos\theta \tag{30b}$$

$$\dot{y} = v\sin\theta \tag{30c}$$

$$\dot{v} = g\sin\theta \tag{30d}$$

$$x(0) = y(0) = 0, x(T) = -y(T) = 1 \tag{30e}$$

$$g = -9.81 \tag{30f}$$

$$x + y \geq -1.5 \tag{30g}$$

where θ is the control.

By applying ICRM, the path constraint was incorporated into the problem without the complexities mentioned in Section I. The trajectory remains a single arc that never violates the path constraint. As the regularization parameter (ϵ) is decreased to 10^{-6}, the trajectory is seen to follow the path constraint very well as shown in Figure **??**, while still minimizing the total time, T.

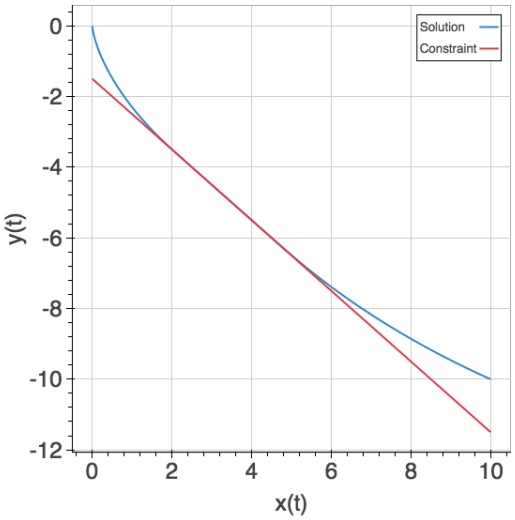

Figure 1. Solution for constrained Brachistochrone problem

B. Maximum Terminal-Energy Hypersonic Trajectories with Heat Rate Constraint

To demonstrate that ICRM can be applied to more complex aerospace problems, a scenario involving maximum terminal energy trajectories of a slender hypersonic vehicle is examined. The vehicle is assumed to be capable of angle-of-attack control, and having a peak L/D of around 2.4. The boundary conditions and the environment parameters are listed in Tables 1 and 2 respectively.

The problem is defined as follows:

$$\text{Max } v(T)^2 \tag{31a}$$
$$\text{Subject to :}$$
$$\dot{h} = v\sin\gamma \tag{31b}$$
$$\dot{\theta} = \frac{v\cos\gamma}{r} \tag{31c}$$
$$\dot{v} = \frac{-D}{m} - \frac{\mu\sin(\gamma)}{r^2} \tag{31d}$$
$$\dot{\gamma} = \frac{L}{mv} + \left(\frac{v}{r} - \frac{\mu}{vr^2}\right)\cos(\gamma) \tag{31e}$$

$$\begin{aligned} r &= R_E + h \\ D &= qC_D A_{ref} \\ L &= qC_L A_{ref} \\ q &= \frac{1}{2}\rho v^2 \\ \rho &= \rho_0 \exp(-h/h_s) \\ \\ C_L &= C_{L1}\alpha + C_{L0} \\ C_D &= C_{D2}\alpha^2 + C_{D1}\alpha + C_{D0} \end{aligned} \tag{31f}$$

Table 1. Post-boost staging and impact conditions.

State	*Staging (t=0)*	*Impact (t=T)*
h	80,000 m	0 m
V	4000 m/s	free
γ	-45 deg	free
θ	0 deg	1 deg

Table 2. Environment Parameters.

Parameter	Value
μ	$3.986\text{e}14\,\text{m}^3/\text{s}^2$
R_E	$6.378\text{e}6\,\text{m}$
ρ_0	$1.2\,\text{kg}/\text{m}^3$
h_s	7,500 m

A stagnation point heat rate constraint is applied to the problem defined in Eqs. (31). The heat rate is computed using the Sutton-Graves convective heating equations[21] as shown in Eq. (32).

$$\dot{Q} = k\sqrt{\frac{\rho}{r_n}}v^3, k = 1.74153 \times 10^{-4} \text{ for Earth} \tag{32}$$

The problem was solved in multiple steps using a continuation process with each step using the prior solution as the initial guess. The one-sided saturation function in Eq. (23) is chosen to regularize the constraint using ICRM. The problem was initially solved with $\dot{Q}_{max}$ set to 10,000 W/cm^2 which makes the constraint inactive. The regularization parameter ϵ was set to 10^{-2}. Figure 2 shows the results of changing $\dot{Q}_{max}$ from 10,000 W/cm^2 (blue) to 1,200 W/cm^2 (red). As the constraint limit is decreased, the vehicle is forced to fly higher in the atmosphere in order to reduce the amount of heat experienced. It can be seen that the actual peak heat flux $\dot{Q}$ in Fig. 2(b) in the final trajectory is around 900 W/cm^2, much lower than the actual constraint of 1,200 W/cm^2. This is due to the push-off factor induced by high value of ϵ. Decreasing the magnitude of epsilon (as shown in the next example), results in a smaller push-off factor.

After changing $\dot{Q}_{max}$ to the desired value, continuation is performed on the regularization parameter, ϵ. Fig. 3 shows the results of changing ϵ from 0.01 (blue) to 10^{-6} (red) which reduces the push-off factor and brings the trajectories closer to the constraint. As the push-off factor is reduced, the vehicle flies lower in the atmosphere (Fig. 3(a)) as the effective limit on the peak heating rate is increased. As ϵ is decreased, the actual heating rate saturates at the constraint limit of 1,200 W/cm^2 at its peak. Unlike in conventional optimal control theory, this complete trajectory is still one arc, and the boundary value problem is still a two-point boundary value problem rather than a multi-point boundary value problem.

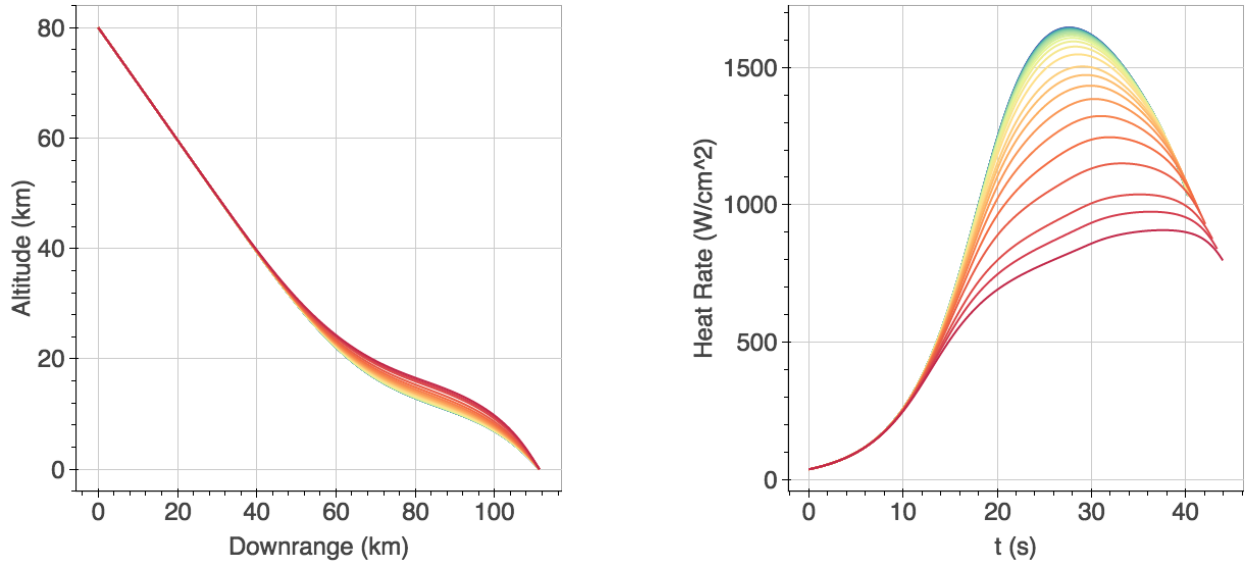

(a) Altitude-Downrange (b) $\dot{Q}$ vs Time

Figure 2. Heat Rate Constraint – Continuation in $\dot{Q}_{max}$ ($\epsilon = 0.01$)

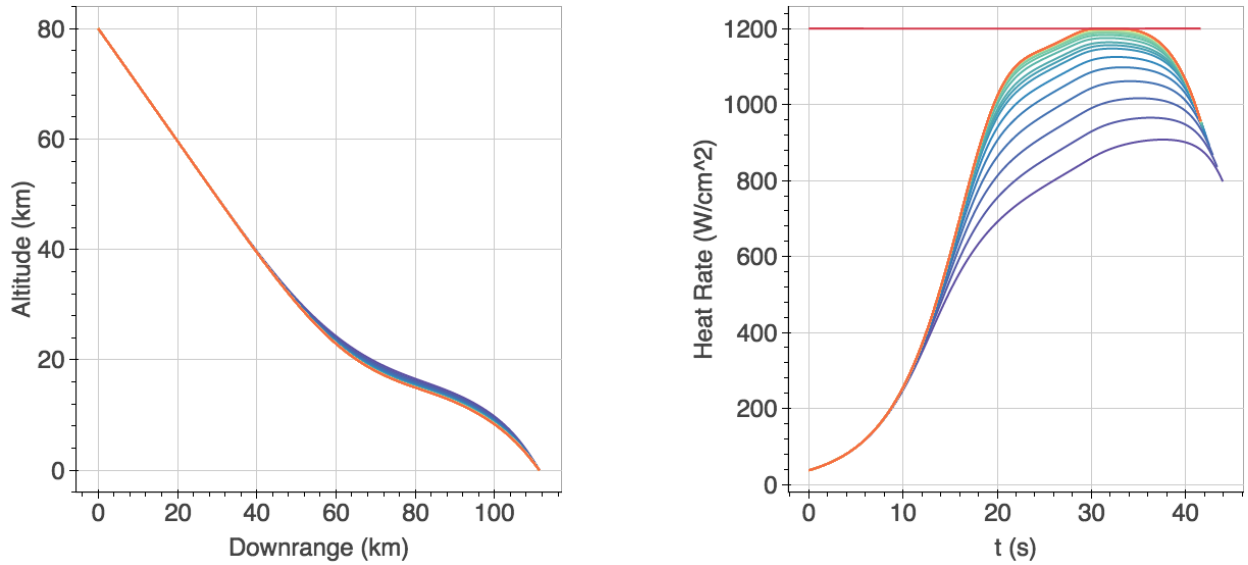

(a) Altitude-Downrange (b) $\dot{Q}$ vs Time

Figure 3. Heat Rate Constraint – Continuation in ϵ from 0.01 to 10^{-6}

1. *Heat Rate and Angle-of-Attack Constraints*

When the hypersonic trajectory problem is formulated as in the last section, there is a side effect that there is no actual limit on the angle-of-attack. For a maximum terminal energy problem, this is not a significant issue as the optimal solution tends to minimize the angle-of-attack.

Figure 4(a) shows the control history for the heat-rate constrained trajectory from the last section. It can be seen that initially, the angle of attack has very high and unrealistic values. This is not too critical as this happens in a phase of the trajectory where there is hardly any atmosphere. However, this can be mitigated by adding a constraint on the angle-of-attack.

Using ICRM, the angle-of-attack constraint can be enforced in the problem simultaneously with the heat rate constraint, and both constraints are satisfied at all points. The normalized angle-of-attack constraint is defined as:

$$-1 \leq \frac{\alpha}{\alpha_{max}} \leq 1 \tag{33}$$

Since this is a two-sided constraint, the saturation function from Eq. (25) is used to implement this constraint in ICRM. The constraint limit, α_{max} is set to 40°. The regularization parameter for the angle-of-attack constraint, ϵ_{alpha} is initially set to 10^{-4}. Figure 4(b) shows the change in control history as ϵ_{alpha} is changed from 10^{-4} (blue) to 10^{-7} (red), reducing the push-off factor and bringing the actual control closer to the constraint.

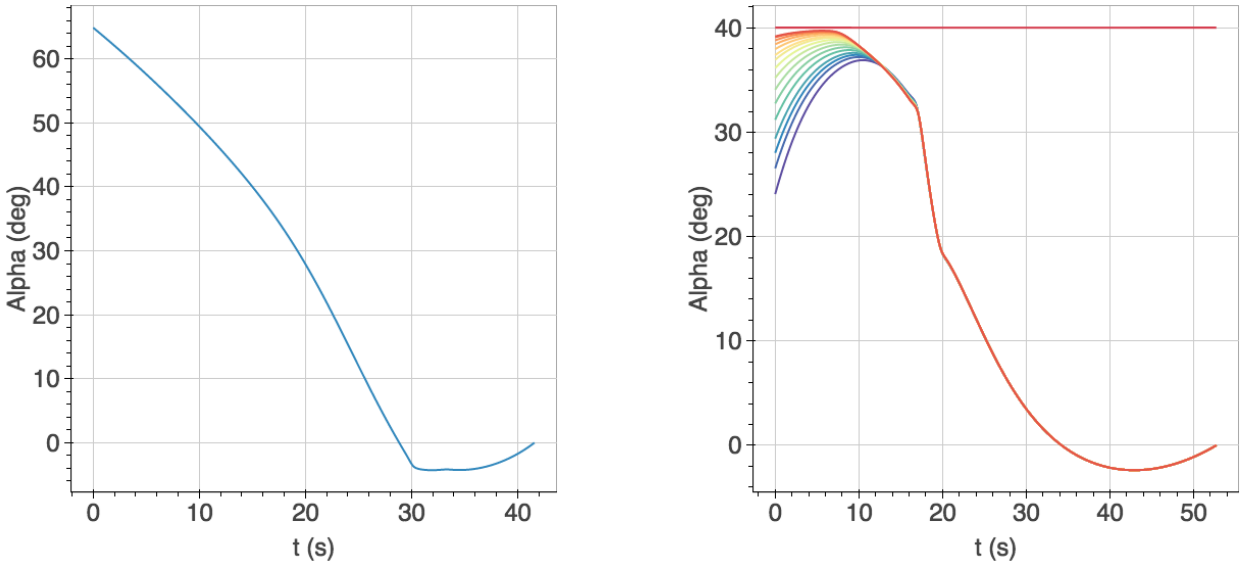

(a) Only Heat Rate constraint

(b) Heat Rate and Angle-of-attack constraint

Figure 4. Heat Rate and AoA Constraint – Control history for optimal trajectory

The addition of the control constraint does not significantly influence the trajectory, since the control saturation occurs in a region with very little dynamic pressure. However, adding this constraint demonstrates that ICRM is capable of solving problems in which more than one path constraint is enforced. Such a problem would be generally considered impractical to solve using conventional indirect methods.

V. Conclusions & Future Work

The Integrated Control Regularization Method (ICRM) has been shown to be a viable process for incorporating path constraints into optimal control problems when using indirect methods. ICRM creates two-point boundary value problems with a few extra states for each constraint, effectively making the BVP bigger. However, this is a reasonable trade-off considering that the alternative is a huge multi-point boundary problem that is highly impractical to solve as the number of constraints increases. ICRM helps to avoid

the challenges conventionally associated with path constraints in indirect methods, such as finding the right sequence of constrained and unconstrained arcs and providing initial guesses for interior boundary conditions.

Regularizing path constraints using ICRM represents a first step towards obtaining high quality solutions for large, highly constrained, trajectory optimization problems which would generally be considered impractical to solve using current state-of-the-art indirect *or* direct methods. Further work is required to validate the method, by comparing the results of ICRM to those obtained using conventional optimal control theory and/or direct methods.

References

[1]Betts, J. T., "Survey of numerical methods for trajectory optimization," *Journal of Guidance, Control, and Dynamics*, Vol. 21, No. 2, 1998, pp. 193–207. 1, 2

[2]Betts, J., *Practical Methods for Optimal Control Using Nonlinear Programming*, Advances in Design and Control, Society for Industrial and Applied Mathematics, 2001. 1, 2

[3]Hargraves, Charles R and Paris, Stephen W, "Direct trajectory optimization using nonlinear programming and collocation," *Journal of Guidance, Control, and Dynamics*, Vol. 10, No. 4, 1987, pp. 338–342. 1

[4]Von Stryk, Oskar, "Numerical solution of optimal control problems by direct collocation," *Optimal Control*, Springer, 1993, pp. 129–143. 1

[5]Grant, M. J. and Braun, R. D., "Rapid Indirect Trajectory Optimization for Conceptual Design of Hypersonic Missions," *AIAA Journal of Spacecraft and Rockets*, 2014, pp. 1–6. 2

[6]Antony, Thomas and Grant, Michael J, "Rapid Indirect Trajectory Optimization on Highly Parallel Computing Architectures," *AIAA Journal of Spacecraft and Rockets*, (in press). 2, 5

[7]Bryson, A. E. and Ho, Y. C., *Applied Optimal Control — Optimization, Estimation, and Control*, Taylor & Francis, 1975. 2

[8]Graichen, K., Kugi, A., Petit, N., and Chaplais, F., "Handling constraints in optimal control with saturation functions and system extension," *Systems & Control Letters*, Vol. 59, No. 11, 2010, pp. 671–679. 2, 4, 5

[9]Longuski, J. M., Guzmán, J. J., and Prussing, J. E., *Optimal Control with Aerospace Applications*, Springer, 2014. 2

[10]Mall, Kshitij and Grant, Michael J, "Epsilon-Trig Regularization Method for Bang-Bang Optimal Control Problems," *AIAA Atmospheric Flight Mechanics Conference*, 2016, p. 3238. 4

[11]Mall, Kshitij and Grant, Michael J, "Trigonomerization of Optimal Control Problems with Bounded Controls," *AIAA Atmospheric Flight Mechanics Conference*, 2016, p. 3244. 4

[12]Gear, C. W. and Petzold, L. R., "ODE methods for the solution of differential/algebraic systems," *SIAM Journal on Numerical Analysis*, Vol. 21, No. 4, 1984, pp. 716–728. 5

[13]Campbell, S. L., "The numerical solution of higher index linear time varying singular systems of differential equations," *SIAM journal on scientific and statistical computing*, Vol. 6, No. 2, 1985, pp. 334–348. 5

[14]Brenan, K. E. and Engquist, B. E., "Backward differentiation approximations of nonlinear differential/algebraic systems," *Mathematics of Computation*, Vol. 51, No. 184, 1988, pp. 659–676. 5

[15]Gear, C. W., "Maintaining solution invariants in the numerical solution of ODEs," *SIAM journal on scientific and statistical computing*, Vol. 7, No. 3, 1986, pp. 734–743. 5

[16]Soares, R. d. P. and Secchi, A. R., "Direct initialisation and solution of high-index DAE systems," *Computer Aided Chemical Engineering*, Vol. 20, 2005, pp. 157–162. 5

[17]Führer, C. and Leimkuhler, B., "Numerical solution of differential-algebraic equations for constrained mechanical motion," *Numerische Mathematik*, Vol. 59, No. 1, 1991, pp. 55–69. 5

[18]Brenan, K., "Stability and convergence of difference approximations for higher index differential/algebraic equations with applications to trajectory control," *PhD Disertation, Math. Dept. UCLA, Los Angeles*, 1983. 5

[19]Lötstedt, P. and Petzold, L., "Numerical solution of nonlinear differential equations with algebraic constraints. I. Convergence results for backward differentiation formulas," *Mathematics of computation*, Vol. 46, No. 174, 1986, pp. 491–516. 5

[20]Petzold, L. and Lötstedt, P., "Numerical solution of nonlinear differential equations with algebraic constraints II: Practical implications," *SIAM Journal on Scientific and Statistical Computing*, Vol. 7, No. 3, 1986, pp. 720–733. 5

[21]Sutton, K. and Graves Jr., R. A., "A general stagnation-point convective heating equation for arbitrary gas mixtures," Tech. rep., National Aeronautics and Space Administration, 1971. 7